Mechatronics 98 (2024) 103120

Contents lists available at ScienceDirect

Mechatronics

journal homepage: www.elsevier.com/locate/mechatronics

Real-time estimation of longitudinal tire stiffness considering dynamic characteristics of tire☆

Jongyong Do [a], Dongyoon Hyun [b], Kyoungseok Han [c,*], Seibum B. Choi [a,*]

[a] Department of Mechanical Engineering, Korea Advanced Institute of Science and Technology, 291 Daehak-ro Yuseong-gu, Daejeon, 34141, Republic of Korea
[b] Hyundai Motor Company, Hyundai-Kia R&D Center, 150 Hyundaiyeonguso-ro Namyang-eup, Hwaseong-si Gyeonggi-do, 18280, Republic of Korea
[c] School of Mechanical Engineering, Kyungpook National University, 80 Daehak-ro Buk-gu, Daegu, 41566, Republic of Korea

ARTICLE INFO

Keywords:
Longitudinal tire stiffness
Tire–road friction coefficient
Tire dynamics
Extended Kalman filter

ABSTRACT

To enhance the effectiveness of active safety control, the tire–road friction coefficient (TRFC) must be precisely estimated, and the longitudinal tire stiffness coefficient is an important vehicle dynamic parameter to estimate TRFC. In this research, we present an observer that improves the performance of longitudinal tire stiffness coefficient estimation by applying tire dynamics that were previously applied in the lateral direction to the longitudinal direction. To begin, we model longitudinal tire dynamics using the relaxation length concept and validate the model using vehicle braking tests. We develop an observer that estimates the longitudinal tire stiffness coefficient by integrating the proposed tire dynamics and vehicle dynamics. The observer, which is based on an extended Kalman filter, can be applied to nonlinear systems and successfully removes noise from wheel speed measurement. The observer's estimation performance is verified using CarSim simulation and vehicle tests, and the results are compared to existing approaches that do not account for longitudinal tire dynamics. Even in the transient section when the vehicle begins accelerating, the difference between the estimate and the reference value is about 0.3% using the proposed method, but if tire dynamics are not taken into account, the estimate is 6.5% lower than the reference value.

1. Introduction

1.1. Research background and motivation

The vehicle interacts with the road surface through its tires only. Tires support the weight of the vehicle and generate longitudinal and lateral forces to control vehicle motion. The maximum force that the tire can transmit is determined by the tire–road friction coefficient (TRFC). The TRFC means the limit of the force that can be transmitted through the tire. Therefore, the vehicle stability can be identified through the TRFC. In addition, the TRFC is especially important when designing active safety systems like Adaptive Cruise Control (ACC), Anti-lock Braking System (ABS), Traction Control System (TCS), and Electronic Stability Control (ESC) since the vehicle dynamic performance is physically limited by the friction coefficient. Without friction information, active safety systems must be operated conservatively to take account of the safety margin. However, unfortunately, the TRFC is not generally given in real-time, and estimation is also challenging [1].

A representative method among TRFC estimation studies is to use the relationship between friction coefficient and longitudinal slip ratio, Fig. 1. Slip is the difference between wheel speed and vehicle speed, and longitudinal slip ratio is calculated by dividing slip by vehicle speed. When the longitudinal slip ratio is small, it is reasonable to assume that the friction coefficient and the longitudinal slip ratio have a linear relationship, and the proportional constant is known as the longitudinal tire stiffness. The TRFC-slip ratio curve has different shapes depending on the condition of the road surface and tires. In Fig. 1, when the TRFC is large, the curve's initial slope and peak value are large, but when the road surface is relatively slippery, the curve's initial slope and peak value are small. Therefore, the TRFC can be estimated using the property that the longitudinal tire stiffness coefficient changes depending on driving conditions. Sensors embedded in mass-produced vehicles have low accuracy and are highly affected by driving noise [2], so it is difficult to guarantee the performance of estimating the longitudinal tire stiffness.

Previous studies on longitudinal tire stiffness estimation commonly use a static tire model. However, the lag effect occurs in the force transmitted to the road surface as a result of the dynamic characteristics of tire. If the tire is a rigid body, the tire force is transmitted

☆ This paper was recommended for publication by Associate Editor Hamid Reza Karimi.

* Corresponding authors.
E-mail addresses: djy0129@kaist.ac.kr (J. Do), dyhyun@hyundai.com (D. Hyun), kyoungsh@knu.ac.kr (K. Han), sbchoi@kaist.ac.kr (S.B. Choi).

https://doi.org/10.1016/j.mechatronics.2023.103120
Received 13 September 2022; Received in revised form 13 November 2023; Accepted 9 December 2023
Available online 22 December 2023

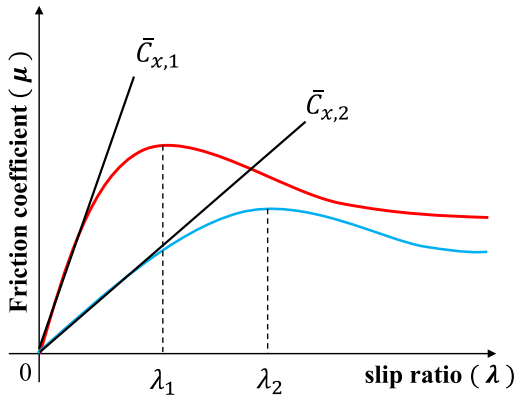

Fig. 1. Tire–road friction coefficient, wheel slip ratio, and longitudinal tire stiffness.

immediately when wheel torque occurs, but the tire actually has elastic properties. When torque is applied to the wheel, the tire gradually deforms and transmits the force. Longitudinal tire dynamics can be modeled using the concept of relaxation length, which is a property of pneumatic tires that describes the lag effect of the steady-state tire force, and the purpose of this study is to improve the real-time longitudinal tire stiffness estimation performance by taking such tire dynamic characteristics into account.

1.2. Literature review

The TRFC estimation have been actively studied in the field of vehicle dynamics. First, there is a method for estimating the TRFC by evaluating the road surface with a vision sensor [3] and another method for determining the degree of moisture content of the road surface with an optical sensor [4]. Using these approaches, the friction coefficient can be estimated in real-time without being limited to driving or braking, and road surface information can be predicted in advance before the vehicle reaches the road surface. Nonetheless, there are limitations, such as the requirement for an additional sensor, a high reliance on sensor performance, and sensitivity to ambient light conditions. The approach of determining the icy road by detecting the ambient temperature has the same problem.

A strain gauge is attached to the tire tread and tire deformation between the center and end of the tire tread is also used to estimate the road friction coefficient [5]. However, it is difficult to implement due of numerous practical concerns such as price, reliability, power supply, signal processing, and wireless sensor connection. The wheel slip-based estimating method avoids the need for extra sensors. However, due to the substantial error in the data collected from the on-board sensor, the estimation performance cannot be guaranteed. As a result, research has been carried out to overcome these difficulties by employing additional sensors such as a global positioning system (GPS) or an inertial measurement unit (IMU) [6–8].

When the longitudinal slip ratio is small, the TRFC tends to be proportional to the longitudinal slip ratio. The initial slope of the TRFC-slip ratio graph is the longitudinal tire stiffness. As a result, attempts have been made to estimate the friction coefficient using the tire stiffness. Most of the studies for estimating the tire stiffness were conducted using the least-squares method based on wheel dynamics and vehicle longitudinal dynamics [1,9–12].

If the tire stiffness is obtained through the linear estimation algorithm [13], the accuracy of the estimation result cannot be guaranteed because it is sensitive to measurement error and road noise [14]. Similarly, the Gauss–Newton method cannot guarantee the convergence of the nonlinear model. Even increasing the number of algorithm iterations does not allow for the correction of all random measurement errors [2]. Therefore, methods for minimizing measurement error by applying a filter or designing an observer were studied [15]. The method using the Kalman filter shows consistent estimation performance by minimizing the effect of noise or disturbance. However, if a model including dynamics is not used, the effect is the same as low-pass filtering [14]. In particular, the degradation of estimation performance in transient regions is noticeable.

1.3. Research objectives and contributions

While research has been conducted in the direction of using additional sensors or minimizing measurement error, robust estimation has not been performed. Despite variances in specific methodologies, prior research generally used a static tire model [16–19]. In reality, when a tire is deformed, it does not immediately reach a steady-state, but exhibits dynamic characteristics. Accordingly, a lag effect occurs in the force transmitted from the tire to the road. Longitudinal tire dynamics can be modeled using the concept of relaxation length [20,21], and this study aims to improve the real-time longitudinal tire stiffness coefficient estimation performance by considering such dynamic characteristics of the tire.

We propose the real-time estimation of the longitudinal tire stiffness strategy, including the lag effect of the tire force due to the tire carcass stiffness. The goal is to reduce the error of the initial estimate in the transient response region with small longitudinal slip ratio, as well as to develop the estimation logic so that the estimate quickly converges to the true value. Through the enhancements made in this study regarding tire stiffness estimation performance, we anticipate achieving the accurate estimation of TRFC, thereby enhancing the performance of active safety control systems.

1.4. Paper structure

The rest of this paper is organized as follows. Section 2 deals with tire dynamic characteristic analysis and tire dynamics modeling through experiments. Section 3 introduces the design of the observer for estimating the longitudinal tire stiffness. In Section 4, the observer's performance is verified through CarSim simulation and experiment. Finally, Section 5 concludes the paper.

2. Modeling of longitudinal tire dynamic characteristics

When a longitudinal force is applied to the tire, the sidewall of the tire is deformed according to the carcass stiffness, but the static tire model does not take these behaviors into account (e.g., Brush model, [22]). The force applied to the tire deforms the carcass which is the part that forms the tire skeleton inside the tread. In this Section, the dynamic properties of tires are modeled and its accuracy is verified considering the carcass stiffness.

2.1. Tire dynamic characteristics

In the conventional static tire model, it is assumed that the longitudinal force due to the deformation of the tire occurs immediately. However, since the tire is indeed not a rigid body, it has dynamic characteristics [23]. Fig. 2 shows the relationship between the friction coefficient and wheel slip ratio when the vehicle accelerates and decelerates in the CarSim simulation. According to the static model, the slip ratio and friction coefficient have a one-to-one correspondence. However, since the slip ratio and friction coefficient do not correspond to one-to-one, it can be expected that there is a dynamic characteristic in the transient section. Because longitudinal deformation occurs in the carcass during vehicle driving and braking, there is a distinction between wheel slip and tread slip in contact with the road surface.

If the deformation appearing in the carcass is h, the longitudinal deformation rate can be expressed as the difference between the wheel slip and the tire tread slip (see Fig. 3). The longitudinal force can

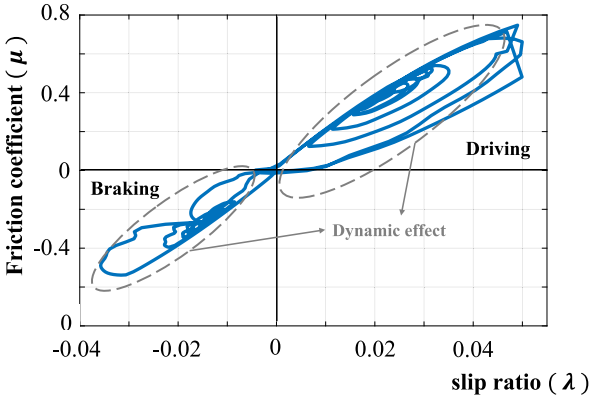

Fig. 2. Effect of tire dynamic characteristics.

be defined in two ways: first, as the product of the longitudinal tire stiffness coefficient and the slip ratio, and second, as the product of the longitudinal carcass stiffness coefficient and the carcass deformation length [24]. Combining these relationships, a first-order differential equation for the carcass deformation is derived as follows [25].

$$V_{x,s} = R_e\omega - V_x \tag{1}$$

$$\frac{dh^L}{dt} = V_{x,s} - V_{x,s}^L \tag{2}$$

where $V_{x,s}$, R_e, ω, V_x, and h are the longitudinal wheel slip speed, the tire effective rolling radius, the wheel speed, the vehicle longitudinal speed, and the carcass deformation. The rate of the carcass deformation dh^L/dt is expressed as the difference between wheel slip speed ($V_{x,s}$) and tire tread slip speed ($V_{x,s}^L$), which includes the dynamic characteristics due to the stiffness of the carcass. That is, the time lag effect between tire–road contact surface and wheel is considered in $V_{x,s}^L$. The superscript L denotes including lag effect.

The longitudinal force applied to the tire can be computed as follows.

$$F_x^L = C_x\lambda^L \tag{3}$$

$$\lambda^L = \frac{V_{x,s}^L}{V_x} \tag{4}$$

where F_x, C_x, and λ are the tire longitudinal force, the longitudinal tire stiffness, and the wheel slip ratio. In Eq. (3), F_x^L is the longitudinal force that causes the lag effect due to the stiffness of the carcass. In general, the linear relationship holds only when the slip rate is small [22]. The tire longitudinal force can also be expressed as the longitudinal stiffness coefficient of the tire carcass and the carcass deformation.

$$F_x^L = K_x h^L \tag{5}$$

where K_x is the longitudinal tire carcass stiffness. h^L represents the carcass deformation, including the lag effect caused by the tire's dynamic characteristics.

Now, the following equations can be derived by rearranging Eqs. (1)–(5).

$$\frac{dh^L}{dt} + \frac{K_x}{C_x}V_x h^L = V_{x,s} \tag{6}$$

$$\sigma = \frac{C_x}{K_x} \quad : \text{ relaxation length} \tag{7}$$

$$\frac{\sigma}{V_x}\frac{dh^L}{dt} + h^L = \frac{C_x}{K_x}\frac{V_{x,s}}{V_x} = \frac{C_x\lambda}{K_x} = \frac{F_x}{K_x} \tag{8}$$

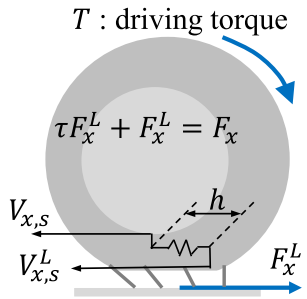

Fig. 3. Tire Carcass compliance Model.

The relaxation length is defined as the value obtained by dividing the longitudinal tire stiffness coefficient by the longitudinal carcass stiffness coefficient in the first differential equation for carcass deformation h. The relaxation length is the distance traveled by the vehicle from the start of the tire's deformation to the steady state. In the first-order differential equation, dividing the relaxation length by the vehicle speed results in a time constant. Since the carcass stiffness coefficient, K_x is an inherent characteristic of a tire, it can be considered as a constant. The longitudinal tire stiffness coefficient C_x is a variable because the relation of the longitudinal force to wheel slip varies depending on the road condition. Eq. (8) can be simplified using a time constant τ and expressed as Eq. (9) below.

$$\tau\frac{dh^L}{dt} + h^L = \frac{F_x}{K_x}, \qquad \tau = \frac{\sigma}{V_x} \tag{9}$$

According to Eq. (5), the dynamics for the longitudinal force can be expressed as follows.

$$\tau\frac{dF_x^L}{dt} + F_x^L = F_x, \qquad \tau = \frac{\sigma}{V_x} \tag{10}$$

Because of the aforementioned dynamics, longitudinal forces are not transferred immediately in driving and braking situations. As a result, when a static tire model is used, the estimation error will be large. In contrast, the developed model in (10) can consider a such lag effect of the pneumatic tires, resulting in the improvement model accuracy.

2.2. Model verification

Through the vehicle experiments, the dynamic characteristics of the tire under braking conditions were analyzed in this subsection. The Hyundai Tucson was utilized as a test vehicle. The longitudinal slip ratio was calculated by measuring the longitudinal speed of the vehicle using RT3002 and the angular velocity of the driving wheel using ABS wheel sensor, and the friction coefficient was calculated by measuring the longitudinal force and vertical load applied to the tire using a wheel force transducer.

$$\mu = \frac{F_x}{F_z} \tag{11}$$

where μ and F_z are the TRFC and the tire vertical load.

The scenario is set up so that the vehicle travels straight at 70 km/h before decelerating to 0.7 g. The vehicle used in the experiment is a front-wheel-drive system. The transfer function between the longitudinal force and the slip ratio can be expressed as follows.

$$\frac{F_x^L(s)}{\lambda(s)} = \frac{C_x}{\frac{\sigma}{V_x}s + 1} \tag{12}$$

The relaxation length was calculated using the measured values of F_x and λ, and it was found that $\sigma = 0.5$ m. And the friction coefficient (longitudinal force) data were corrected using the time constant $\tau = \sigma/V_x$ that varies according to the speed. A linear regression method is used to minimize cost function J(13), and $\overline{C}_x$ is the normalized value

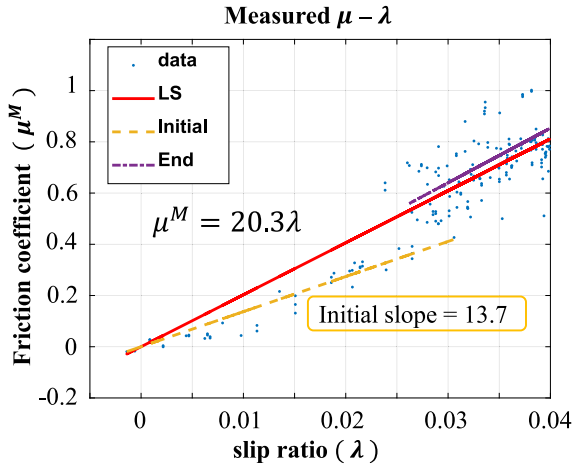

Fig. 4. Estimation result using static model.

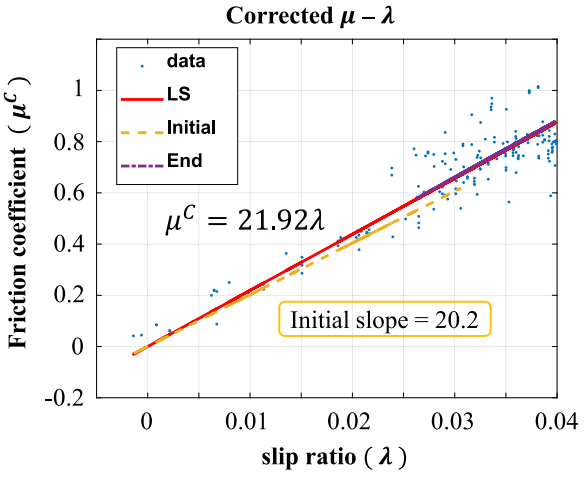

Fig. 5. Estimation result using the developed dynamic tire model.

by dividing C_x by the tire vertical load. $\overline{C}_x$ is a constant independent of tire vertical load, and the longitudinal tire stiffness coefficient estimated in this study is $\overline{C}_x$ rather than C_x. The longitudinal tire stiffness coefficient $\overline{C}_x$ is calculated from the initial slope of the friction coefficient–slip ratio graph.

$$J = (\mu - \overline{C}_x \lambda)^2 \tag{13}$$

In Fig. 4, the slope is obtained by applying the least squares method to the friction coefficient and wheel slip ratio calculated using only the measured values without correction by tire dynamics. The red solid line (LS) is the result of applying the least squares method to all data in the transient region until the slip ratio reaches the steady state. The yellow dashed line (Initial) is the result of applying the least squares method only to data with a small slip ratio, and the purple dash-single dotted line (End) is the result of applying the least squares method only to the data with a large slip ratio. The most notable point is that the difference between the LS slope and the Initial slope is large, while the LS slope and the End slope is similar. If dynamics does not exist, the LS slope, the Initial slope, and the End slope should be similar regardless of the range of the slip ratio.

In Fig. 5, the slope is obtained by applying the least squares method to the friction coefficient corrected by tire dynamics modeled above and wheel slip ratio. It can be seen that the difference between LS slope 21.92 and Initial slope 20.2 is relatively small compared to Fig. 4, and the LS slope and end slope are almost identical. Therefore, it can be concluded that the initial estimation performance of longitudinal tire stiffness coefficient can be improved by considering tire dynamics. It also can be seen that the data convergence for the linear regression-estimated straight line has improved.

Table 1
Tire dynamics effect verification experiment results.

	$\overline{C}_x$	RMSE	R^2
w/o Tire dynamics	20.3	0.1065	0.827
w/ Tire dynamics	21.92	0.0859	0.853

In Table 1, the estimated normalized longitudinal tire stiffness increases by 7.98% from 20.3 to 21.92 before and after considering tire dynamics. Root mean square error (RMSE) measures prediction accuracy by calculating the square root of the average squared differences between predicted and actual values. Lower RMSE values indicate better model performance. R^2 is a statistical measure that represents the proportion of the variance in the dependent variable that is explained by the independent variables in a regression model. It ranges from 0 to 1, with higher values indicating a better fit of the model to the data. Before considering the tire dynamics, the R^2 for the estimated straight line was 0.827, but after considering the tire dynamics, the R^2 for the estimated straight line is 0.853, which is slightly larger. Consequently, the RMSE decreases as well, from 0.1065 to 0.0859. If the tire stiffness coefficient can be accurately estimated from the low slip section, the data from the transient region can be used to determine road friction.

3. System modeling

In this study, it is postulated that vehicle specifications, such as vehicle mass, wheelbase, width, and aerodynamic coefficients, as well as the vehicle's center of gravity, are known. Because there are limitations to estimating brake torque accurately, this study focuses solely on the driving situation [26]. In the case of regenerative braking in an electric vehicle, it is possible to design an estimation logic in a braking situation because the braking torque can be found through the motor torque.

3.1. Longitudinal vehicle and tire dynamics

$$\dot{\omega} = \frac{T - R_e F_x - M}{I} \tag{14}$$

$$m\dot{V}_x = 2F_x - bV_x{}^2 - F_{rr} \tag{15}$$

$$\frac{\sigma}{V_x}\frac{dF_x^L}{dt} + F_x^L = F_x \tag{16}$$

where T, I, M, m, b, and F_{rr} are the wheel torque, the wheel moment of inertia, the loss torque due to rolling resistance, the vehicle mass, air resistance related coefficient, and the rolling resistance. In the above equations, wheel dynamics, vehicle longitudinal dynamics, and tire dynamics are represented in the order given. The TRFC and the wheel slip ratio are calculated as shown in Eqs. (17) and (18).

$$\mu = \frac{F_x}{F_z} = \overline{C}_x \lambda \tag{17}$$

$$\lambda = \frac{R_e\omega - V_x}{V_x} \tag{18}$$

The tire vertical load F_z is expressed in consideration of the load transfer due to the acceleration of the vehicle. The vertical load on the vehicle's right front tire is depicted in Eq. (19) [27].

$$F_{z,FR} = mg\left(\frac{l_r}{L} - \frac{h_{cg}}{Lg}\frac{2F_{x,FR} - bV_x^2 - F_{rr}}{m}\right)\frac{d_l}{D} - \frac{bV_x^2}{L} \tag{19}$$

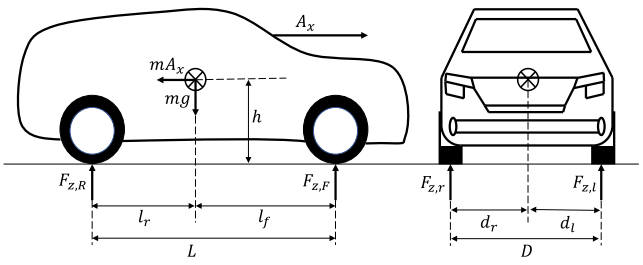

Fig. 6. Side view and front view showing the vehicle parameters from the center of gravity.

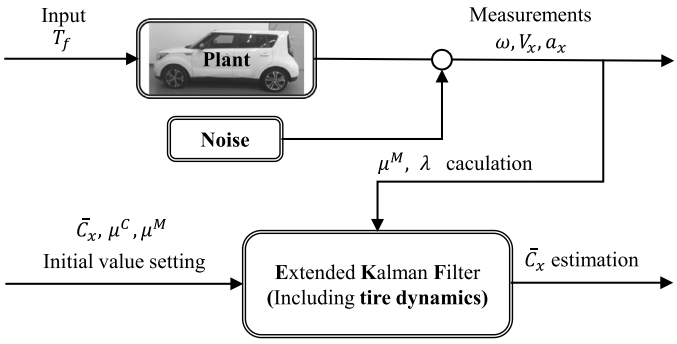

Fig. 7. Overview of the estimation strategy.

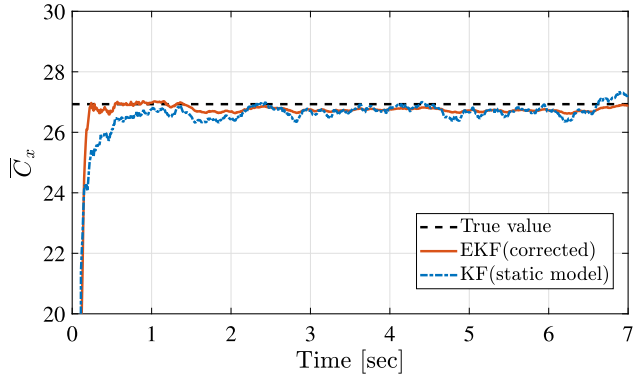

Fig. 8. Estimation result of $\bar{C}_x$ (simulation, $\mu = 1$).

where L, D, and h_{cg} are the wheel base, the vehicle width, and the vehicle center of gravity height. The vehicle's center of gravity is shown in Fig. 6. Since the longitudinal tire stiffness coefficient changes due to load transfer, a normalized value ($\bar{C}_x$) is used by dividing the longitudinal tire stiffness coefficient by the tire vertical load.

Plant modeling is done using the three mentioned above dynamics, and it is modeled as a nonlinear system. The three states are the longitudinal tire stiffness coefficient $\bar{C}_x$, TRFC μ^C corrected by tire dynamics, and TRFC μ^M calculated from measured values [28,29]. The output values measured by the sensor are the wheel slip ratio λ and the TRFC μ^M (dynamics are not taken into account).

3.2. Tire stiffness estimation strategy

From the wheel slip ratio $\lambda = \dfrac{R_e\omega - V_x}{V_x}$, the effective rolling radius R_e is calculated to satisfy the relationship $V_x = R_e\omega$ when the vehicle is moving at a constant velocity. The state vector of the system is defined as $x \in \mathbb{R}^3$, where x consists of $\bar{C}_x$, μ^C, and μ^M. This is a form of augmented observer that includes the parameter to be estimated in the state. It is a kind of adaptation that performs parameter estimation using a known model structure. λ is included in output y because $\bar{C}_x$ can be accurately estimated only when noise included in the wheel slip ratio is effectively removed by filtering. The system is nonlinear and is denoted by f(x) and h(x). Here, w and v are the process and measurement noises and both are zero-mean additive white Gaussian noise. The system form is the following Eqs. (20).

$$\begin{aligned} \dot{x} &= f(x) + w \\ y &= h(x) + v \end{aligned} \qquad x = \begin{bmatrix} \bar{C}_x \\ \mu^C \\ \mu^M \end{bmatrix} \qquad y = \begin{bmatrix} \lambda \\ \mu^M \end{bmatrix} \tag{20}$$

When $x_1 = \bar{C}_x, x_2 = \mu^C, x_3 = \mu^M, f(x)$ and $h(x)$ can be expressed as follows.

$$f(x) = \begin{bmatrix} 0 \\ 0 \\ \dfrac{K_x V_x}{F_z}\dfrac{x_2 - x_3}{x_1} \end{bmatrix} \qquad h(x) = \begin{bmatrix} x_2 \\ x_1 \\ x_3 \end{bmatrix} \tag{21}$$

Changes in carcass stiffness coefficient due to tire wear or hardening are not considered. As a state observer, an Extended Kalman Filter (EKF) is used because the plant model is a time-varying nonlinear system [30]. Fig. 7 shows an overview of the longitudinal tire stiffness coefficient estimation strategy using the extended Kalman filter.

In the CarSim simulation or vehicle experiment, the torque applied to the driving wheels (front wheels) is the system input. The wheel angular velocity, the vehicle longitudinal speed, and the longitudinal vehicle acceleration are measured through the Anti-lock Braking System (ABS) wheel sensor, Global Positioning System (GPS), and built-in accelerometer. Since the system is nonlinear as in (21), it is necessary to linearize $f(x)$ and $h(x)$ to update the Kalman gain and calculate the error covariance in real-time. The F and H matrices refer to the Jacobian of $f(x)$ and $h(x)$, respectively.

$$F = \frac{\partial f(x)}{\partial x} = \begin{bmatrix} 0 & 0 & 0 \\ 0 & 0 & 0 \\ -C_1\dfrac{x_2}{x_1^2} + C_1\dfrac{x_3}{x_1^2} & \dfrac{C_1}{x_1} & -\dfrac{C_1}{x_1} \end{bmatrix}, C_1 = \frac{K_x V_x}{F_z} \tag{22a}$$

$$A = I + F \times T \tag{22b}$$

$$H = \frac{\partial h(x)}{\partial x} = \begin{bmatrix} -\dfrac{x_2}{x_1^2} & \dfrac{1}{x_1} & 0 \\ 0 & 0 & 1 \end{bmatrix} \tag{22c}$$

where the matrix A is the result of discretizing matrix F with a sampling time interval T. The extended Kalman filter's algorithm is shown below [30].

$$\hat{x}_k^- = f(\hat{x}_{k-1}) \tag{23a}$$

$$P_k^- = AP_{k-1}A^T + Q \tag{23b}$$

$$K_k = P_k^- H^T (H P_k^- H^T + R)^{-1} \tag{23c}$$

$$\hat{x}_k = \hat{x}_k^- + K_k(z_k - h(\hat{x}_k^-)) \tag{23d}$$

$$P_k = P_k^- - K_k H P_k^- \tag{23e}$$

where P is the error covariance and K is the Kalman gain, which is adjusted at every step. '-' means prediction and '$\wedge$' means estimation.

4. Test results

4.1. Simulation

The simulation proceeds with CarSim, which reflects the real vehicle's dynamic properties well. The target vehicle is a front-wheel-drive vehicle, and all vehicle specifications required by the estimation logic are assumed to be known. The scenario is set up in such a way that the vehicle accelerates while driving straight on flat ground. The maximum coefficient of friction on the road is set to one (i.e., dry asphalt). The sampling time is set to 10 ms, and the acceleration magnitude is fixed

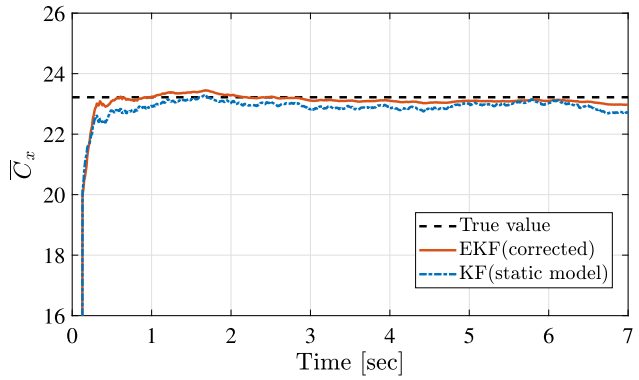

Fig. 9. Estimation result of $\overline{C}_x$ (simulation, $\mu = 0.5$).

Table 2
Vehicle parameters used in the experiment.

Symbol	Description	Value
m	Vehicle mass	1,614 kg
$R_{e,front}$	Effective rolling radius of the drive wheel	0.3086 m
L	Wheel base	2.57 m
D	Vehicle width	1.56 m
h_{cg}	Vehicle center of gravity height	0.565 m
K_x	Carcass longitudinal stiffness coefficient	140,000 N/m

at 0.15 g. To reflect the real-world drivings, Random white noise is applied with a maximum error of 1% for wheel angular speed and vehicle speed, and a maximum error of 5% for vehicle acceleration. Fig. 8 is the result of estimating the $\overline{C}_x$ using the extended Kalman filter designed in Section 3. The true value of $\overline{C}_x$ in the simulation is 26.93, which is revealed by the simulations with the same vehicle model in CarSim.

In Fig. 8, KF is the result of estimating the longitudinal tire stiffness coefficient by applying the Kalman filter to the linear system without considering the tire dynamics [14]. The error range of KF is −2.3 to +1.56%, which is larger than the error range of EKF(including tire dynamics) −1.15 to 0%. It can be seen that the EKF has higher estimation accuracy and faster convergence speed compared to the KF. In EKF considering tire dynamics, relaxation length $\sigma = 0.9\,\text{m}$ and $K_x = 100,000\,\text{N/m}$ from $\sigma = \dfrac{C_x}{K_x}$.

Fig. 9 is the estimation result when $\mu = 0.5$ and is similar to Fig. 8, the estimation result when $\mu = 1$. In this low μ case, the true value of $\overline{C}_x$ is 23.22, which is relatively small because the road friction coefficient is reduced. However, the fact that the EKF shows better performance than the KF does not change.

4.2. Experiment

In this section, experiment is conducted to verify whether the proposed $\overline{C}_x$ estimation method can be applied to real vehicles. In Fig. 11, the Kia Soul EV which is a front-wheel-drive electric vehicle was utilized as a test vehicle. The parameters of this vehicle are shown in Table 2. The vehicle's position, speed, and acceleration are acquired using RT-3002, and wheel speed is measured using an ABS wheel sensor. The motor torque is measurable and the torque applied to the driving wheel can be calculated. Vehicle specifications required for estimation logic are known values, such as vehicle mass, effective rolling radius of front wheels, the center of gravity information, air resistance-related coefficients, and wheel moment of inertia. The experiment is conducted on the flat ground and a road surface with a sufficiently large TRFC (High μ). The sampling time is set to 10 ms. The experimental scenario is a situation in which a driving torque is constantly applied to a vehicle traveling in a straight line. The magnitude of the acceleration is about 0.1 g, which is the degree that general drivers smoothly accelerate in driving daily. The test data are shown in Fig. 10. The steering wheel

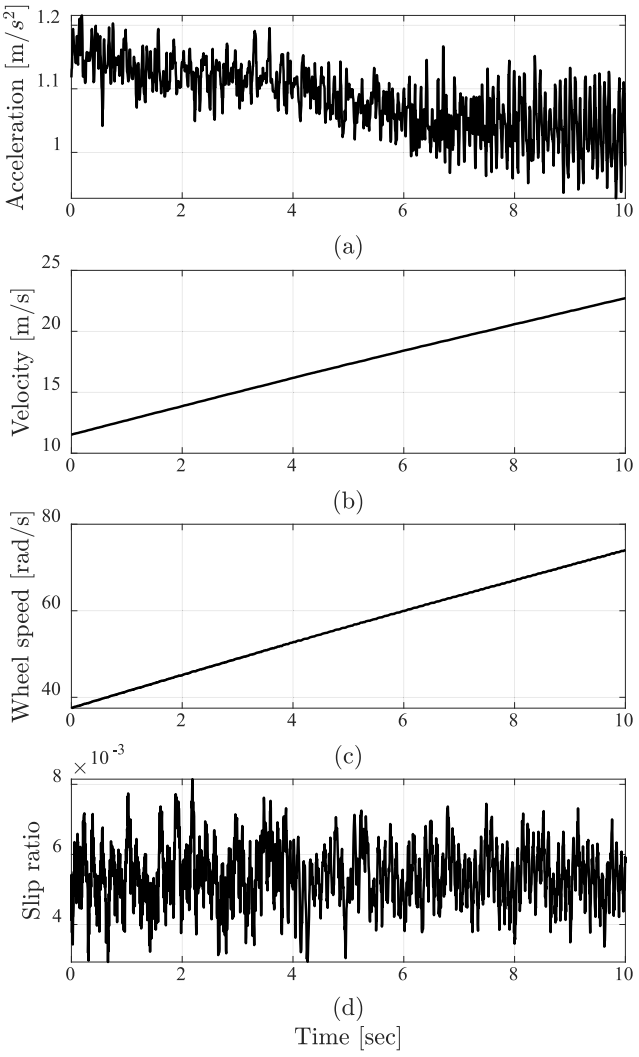

Fig. 10. Vehicle experiment data. (a) longitudinal acceleration; (b) longitudinal velocity; (c) angular velocity of the drive wheel; (d) longitudinal wheel slip ratio.

Fig. 11. Experimental set-up. (a) Test vehicle; (b) RT-3002 for verification.

is neutral and only longitudinal slip occurs. The vehicle accelerates from about 40 km/h to 80 km/h, and the vehicle's acceleration is almost constant at 1 m/s^2. Slip ratio measurements are noisy and this limitation must be overcome with proper filter design.

When estimating without taking tire dynamics into account, the Kalman filter (KF) is used, as it was in the previous simulation. The plant model of the Kalman filter can be expressed as Eq. (24) below.

$$\begin{aligned} \dot{x} &= Fx + w \\ y &= Hx + v \end{aligned} \qquad x = \begin{bmatrix} \dfrac{1}{\overline{C}_x} \end{bmatrix} \qquad y = \lambda = \frac{\mu}{\overline{C}_x} = \mu x \tag{24}$$

The reciprocal of the longitudinal tire stiffness coefficient is set as a state variable, and measurements of the TRFC and wheel slip ratio are

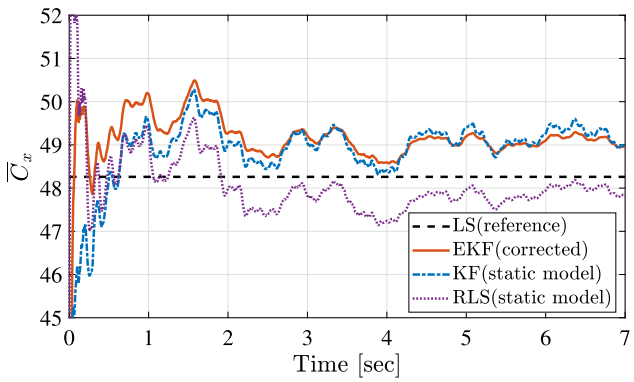

Fig. 12. Estimation result of longitudinal tire stiffness coefficient (experiment).

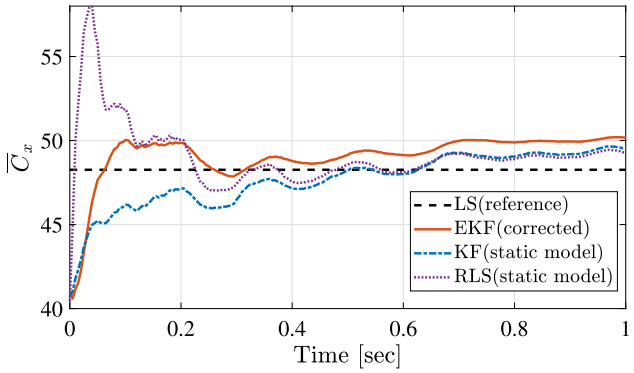

Fig. 13. Estimation performance for the initial phase.

fed into the Kalman filter. When tire dynamics are taken into account, the plant model becomes non-linear, as shown in Eq. (21), and the TRFC is corrected when a transient response appears via the relaxation length concept included in the extended Kalman filter (EKF). In both cases, the estimated results are compared and shown in Fig. 12.

In addition to EKF and KF, the results for the least squares method (LS) and the recursive least squares method (RLS) are also presented as alternative estimation strategies in Fig. 12 and Fig. 13 [30]. The LS is the result of applying the least squares method to all data until the wheel slip reaches a steady state, and is obtained off-line to minimize (13) by measuring μ and λ. Therefore, LS is not a true value, but a reference value for comparison with the estimated value. The LS is the average slope in the $\mu - \lambda$ curve. The average slope is less than the initial slope of the $\mu - \lambda$ curve due to the nonlinearity of the curve (Fig. 1). As a result, the actual longitudinal tire stiffness coefficient is expected to be greater than the longitudinal tire stiffness coefficient calculated using the LS. The RLS is a recursive version of LS, and is a method applicable to sequential data measured in real time. At steady state, the convergence value of the RLS is similar to that of the LS. In RLS, a design factor is a forgetting factor which is a value between 0 and 1. In order to reduce the influence of past data and to be able to react sensitively to current data, the forgetting factor should be set small. Conversely, in order to reduce the change in the estimated value due to the current data noise, the forgetting factor should be set large. Therefore, it is important to set the forgetting factor appropriately, and it is usually set to a value between 0.98 and 1. The RLS estimates $\overline{C}_x$ so that (13) is minimized, and the formulas are shown as (25) and (26).

$$G(k) = \frac{1}{p}\left[G(k-1) - \frac{G^2(k-1)\lambda^2(k)}{p + G(k-1)\lambda^2(k)}\right] \tag{25}$$

$$\hat{\overline{C}}_x(k) = \hat{\overline{C}}_x(k-1) + G(k-1)\lambda(k)(\mu(k) - \hat{\overline{C}}_x(k-1)\lambda(k)) \tag{26}$$

where G and p are the update gain and the forgetting factor. When comparing the estimation results in the above Fig. 13, the obvious difference is the initial estimate immediately after acceleration. In the case of the KF using the TRFC calculated by measurement, the initial longitudinal tire stiffness coefficient estimate is 46.17. The initial longitudinal tire stiffness coefficient is 49.51 based on the EKF with the TRFC corrected by tire dynamics. The difference between the estimated longitudinal tire stiffness coefficient before and after considering tire dynamics is 6.75%. Comparing the initial estimate of KF 46.17 with the convergence value of KF 49.39, there is a difference of 6.50%. Comparing the EKF initial estimate 49.51 with the convergence value of EKF 49.36, there is a difference of only 0.3%. EKF outperforms KF in terms of convergence. Taking into consideration tire dynamics allows for the enhancement of the estimation performance of the longitudinal tire stiffness coefficient. As a result, by improving the performance of estimating the longitudinal tire stiffness coefficient at the initial stage of acceleration, the TRFC will be obtained quickly and accurately. In order to more reliably verify the estimated performance of the proposed observer, the actual value of the longitudinal tire stiffness coefficient must be obtained. If it is shown that vehicle control performance can be improved using the estimated results, the practical value will become more certain.

5. Conclusion

In the case of acceleration/deceleration, deformation occurs in the sidewall of the tire due to the inertia of the wheel. The relaxation length, which is the distance traveled by the vehicle until the tire's deformation reaches a steady state, is used to model tire dynamics. The linearity of the initial data of the TRFC-slip ratio curve increases as the modeled tire dynamics are applied to vehicle braking experiment data. When the longitudinal tire stiffness coefficient is obtained by applying the least-squares method, the RMSE is also reduced.

The observer is intended to effectively remove the noise contained in the wheel slip ratio. The extended Kalman filter is employed as an observer to estimate the longitudinal tire stiffness coefficient since the plant model is nonlinear and has a property that varies in real-time. The performance of the designed observer is verified through CarSim simulation and vehicle experiment, and compared with the method not considering tire dynamics. The proposed method has the advantage of being faster to estimate and has better convergence. The estimated tire stiffness is expected to improve the performance of the active safety control.

CRediT authorship contribution statement

Jongyong Do: Conceptualization, Methodology, Software, Validation, Formal analysis, Investigation, Resources, Data curation, Writing – original draft, Writing – review & editing, Visualization. **Dongyoon Hyun:** Methodology, Software, Validation, Investigation, Resources, Data curation, Supervision, Project administration. **Kyoungseok Han:** Resources, Data curation, Writing – review & editing. **Seibum B. Choi:** Conceptualization, Methodology, Writing – review & editing, Supervision, Project administration, Funding acquisition.

Declaration of competing interest

The authors declare that they have no known competing financial interests or personal relationships that could have appeared to influence the work reported in this paper.

Data availability

The data that has been used is confidential.

Acknowledgments

This study was partly supported by the BK21 FOUR Program of the National Research Foundation Korea (NRF) grant funded by the Ministry of Education, Autonomous Driving Technology Development Innovation Program (20018181; Development of Lv. 4+ Autonomous Driving Vehicle Platform based on Point-to-point Driving to Logistic Center for Heavy Trucks) funded by the Ministry of Trade, Industry & Energy (MOTIE, Korea) and Korea Evaluation Institute of Industrial Technology (KEIT), the National Research Foundation of Korea (NRF) grant funded by the Korean government (MSIP) (No. 2020R1A2B5B01001531), and the Technology Innovation Program (20014983; Development of Autonomous Chassis Platform for a Modular Vehicle) funded by the Ministry of Trade, Industry & Energy(MOTIE, Korea).

References

[1] Han K, Lee E, Choi M, Choi SB. Adaptive scheme for the real-time estimation of tire-road friction coefficient and vehicle velocity. IEEE/ASME Trans Mechatronics 2017;22(4):1508–18.
[2] Carlson CR, Gerdes JC. Consistent nonlinear estimation of longitudinal tire stiffness and effective radius. IEEE Trans Control Syst Technol 2005;13(6):1010–20.
[3] Holzmann F, Bellino M, Siegwart R, Bubb H. Predictive estimation of the road-tire friction coefficient. In: 2006 IEEE conference on computer aided control system design, 2006 IEEE international conference on control applications, 2006 IEEE international symposium on intelligent control. IEEE; 2006, p. 885–90.
[4] Sato Y, Kobayashi D, Watanabe K, Watanabe K, Kuriyagawa Y, Kuriyagawa Y. Study on recognition method for road friction condition. 38, (2):2007, p. 51–6.
[5] Eichhorn U, Roth J. Prediction and monitoring of tyre/road friction. In: XXIV fisita congress, 7-11 June 1992, London. held at the automotive technology servicing society. technical papers. safety, the vehicle and the road. volume 2 (IMECHE NO C389/321 and FISITA NO 925226). 1992.
[6] Miller SL, Youngberg B, Millie A, Schweizer P, Gerdes JC. Calculating longitudinal wheel slip and tire parameters using GPS velocity. In: Proceedings of the 2001 American control conference. (Cat. No. 01CH37148). Vol. 3, IEEE; 2001, p. 1800–5.
[7] Han KS, Lee E, Choi S. Estimation of the maximum lateral tire-road friction coefficient using the 6-DoF sensor. In: 2015 15th international conference on control, automation and systems (ICCAS). IEEE; 2015, p. 1734–8.
[8] Han K, Hwang Y, Lee E, Choi S. Robust estimation of maximum tire-road friction coefficient considering road surface irregularity. Int J Automot Technol 2016;17(3):415–25.
[9] Wang J, Alexander L, Rajamani R. Friction estimation on highway vehicles using longitudinal measurements. J Dyn Sys Meas Control 2004;126(2):265–75.
[10] Lee C, Hedrick K, Yi K. Real-time slip-based estimation of maximum tire-road friction coefficient. IEEE/ASME Trans Mechatron 2004;9(2):454–8.
[11] Mu¨ller S, Uchanski M, Hedrick K. Estimation of the maximum tire-road friction coefficient. J Dyn Sys Meas Control 2003;125(4):607–17.
[12] Han K, Choi M, Choi SB. Estimation of the tire cornering stiffness as a road surface classification indicator using understeering characteristics. IEEE Trans Veh Technol 2018;67(8):6851–60.
[13] Carlson CR, Gerdes JC. Identifying tire pressure variation by nonlinear estimation of longitudinal stiffness and effective radius. In: Proceedings of AVEC 2002 6th international symposium of advanced vehicle control. 2002.
[14] Gustafsson F. Slip-based tire-road friction estimation. Automatica 1997;33(6):1087–99.
[15] Ahn C, Peng H, Tseng HE. Robust estimation of road frictional coefficient. IEEE Trans Control Syst Technol 2011;21(1):1–13.
[16] Bakker E, Nyborg L, Pacejka HB. Tyre modelling for use in vehicle dynamics studies. SAE Trans 1987;190–204.
[17] Kissai M, Monsuez B, Tapus A, Martinez D. A new linear tire model with varying parameters. In: 2017 2nd IEEE international conference on intelligent transportation engineering (ICITE). IEEE; 2017, p. 108–15.
[18] Singh KB, Taheri S. Estimation of tire–road friction coefficient and its application in chassis control systems. Syst Sci Control Eng 2015;3(1):39–61.
[19] Bhoraskar A, Sakthivel P. A review and a comparison of Dugoff and modified Dugoff formula with Magic formula. In: 2017 international conference on nascent technologies in engineering (ICNTE). IEEE; 2017, p. 1–4.
[20] Vantsevich VV, Gray JP. Relaxation length review and time constant analysis for agile tire dynamics control. In: International design engineering technical conferences and computers and information in engineering conference. Vol. 57106, American Society of Mechanical Engineers; 2015, V003T01A038.
[21] Lee E, Lee J, Choi SB. String tyre model for evaluating steering agility performance using tyre cornering force and lateral static characteristics. Veh Syst Dyn 2017;55(2):231–43.
[22] Pacejka H. Tire and vehicle dynamics. Elsevier; 2005.
[23] Clover C, Bernard J. Longitudinal tire dynamics. Veh Syst Dyn 1998;29(4):231–60.
[24] Mavros G. Contact mechanics of tyre–road interactions and its role in vehicle shuffle. In: Tribology and dynamics of engine and powertrain. Elsevier; 2010, p. 703–34.
[25] Rill G. First order tire dynamics. In: Proceedings of the III european conference on computational mechanics solids, structures and coupled problems in engineering, Lisbon, Portugal. Vol. 58, 2006.
[26] Han K, Choi SB, Lee J, Hyun D, Lee J. Accurate brake torque estimation with adaptive uncertainty compensation using a brake force distribution characteristic. IEEE Trans Veh Technol 2017;66(12):10830–40.
[27] Jeong D, Kim S, Lee J, Choi SB, Kim M, Lee H. Estimation of tire load and vehicle parameters using intelligent tires combined with vehicle dynamics. IEEE Trans Instrum Meas 2020;70:1–12.
[28] Cordeiro RA, Victorino AC, Azinheira JR, Ferreira PA, de Paiva EC, Bueno SS. Estimation of vertical, lateral, and longitudinal tire forces in four-wheel vehicles using a delayed interconnected cascade-observer structure. IEEE/ASME Trans Mechatronics 2019;24(2):561–71.
[29] Doumiati M, Victorino AC, Charara A, Lechner D. Onboard real-time estimation of vehicle lateral tire–road forces and sideslip angle. IEEE/ASME Trans Mechatronics 2010;16(4):601–14.
[30] Simon D. Optimal state estimation: Kalman, H infinity, and nonlinear approaches. John Wiley & Sons; 2006.

Jongyong Do received his B.S. and M.S. degrees in mechanical engineering from Korea Advanced Institute of Science and Technology (KAIST), Daejeon, Korea, where he is currently working toward his Ph.D. degree. His research interests include vehicle dynamics, control theory, vehicle motion prediction, and active safety systems.

Dongyoon Hyun received the B.S. and M.S. degrees in agricultural mechanical engineering from Seoul National University, Seoul, Korea. After graduation, he worked five years for the Agency for Defense Development in Korea where he was involved in research and development of army vehicles. He began his graduate studies again in 1996 and received the M.S. and Ph.D. degrees in Mechanical Engineering from Texas A&M University in 1997 and 2001, respectively. Since 2003, he has worked as a Senior Research Engineer at Hyundai-Kia R&D Center.

Kyoungseok Han received the B.S. degree in civil engineering (minor in mechanical engineering) from Hanyang University, Seoul, South Korea, in 2013, and the M.S. and Ph.D. degrees in mechanical engineering from the Korea Advanced Institute of Science and Technology (KAIST), Daejeon, South Korea, in 2015 and 2018, respectively. He was a Research Fellow with the University of Michigan from June 2018 to February 2020. In March 2020, he was appointed as an Assistant Professor with the School of Mechanical Engineering, Kyungpook National University. His current research interests include vehicle dynamics and control, autonomous vehicle, battery electric vehicle, optimization, and control theory.

Seibum B. Choi received the B.S. in mechanical engineering from Seoul National University, Seoul, Korea, the M.S. in mechanical engineering from KAIST, Daejeon, Korea, and the Ph.D. in control from the University of California, Berkeley, CA, USA, in 1993. From 1993 to 1997, he was involved in the development of automated vehicle control systems at the Institute of Transportation Studies, University of California. Through 2006, he was with TRW, Livonia, MI, USA, where he was involved in the development of advanced vehicle control systems. Since 2006, he has been faculty in the Mechanical Engineering Department, KAIST, Korea. His current research interests include fuel-saving technology, vehicle dynamics and control, and active safety systems. Prof. Choi is a Member of the American Society of Mechanical Engineers, the Society of Automotive Engineers, and the Korean Society of Automotive Engineers.